

# Pulsed Electrodeposition of Large-Area, Ordered $\text{Bi}_{1-x}\text{Sb}_x$ Nanowire Arrays from Aqueous Solutions

Liang Li, Guanghai Li,\* Yong Zhang, Youwen Yang, and Lide Zhang

Key Laboratory of Materials Physics, Institute of Solid State Physics, Chinese Academy of Sciences, Hefei 230031, People's Republic of China

Received: July 9, 2004; In Final Form: August 27, 2004

Thermoelectric material  $\text{Bi}_{1-x}\text{Sb}_x$  nanowire arrays have been successfully synthesized by pulsed electrochemical deposition from aqueous solutions into porous anodic alumina membranes. X-ray diffraction results show that the as-synthesized nanowires are single-crystalline and have a highly preferential orientation. Scanning electron microscopy and transmission electron microscopy observations indicate that the ordered  $\text{Bi}_{1-x}\text{Sb}_x$  nanowire arrays are high filling and the diameters of the nanowires are modulated by the pulsed time. Energy dispersive spectrometer analysis indicates that the composition of the nanowires can be tuned by changing the solution concentrations.

## Introduction

Recently, there is renewed interest in thermoelectric (TE) materials, because various experimental and theoretical studies have suggested that the thermoelectric efficiencies (ZT) of low-dimensional materials are largely improved as compared with those of the bulk materials.<sup>1–3</sup> Theoretical calculations have indicated that Bi and its related alloys are promising candidates for low-dimensional TE materials at about 100 K,<sup>4,5</sup> and desirable ZT values can be realized for  $\text{Bi}_{1-x}\text{Sb}_x$  nanowires with diameters of about 35–50 nm, depending on the Sb mole fraction,  $x$ .<sup>6,7</sup>  $\text{Bi}_{1-x}\text{Sb}_x$  alloys are among the best n-type low-dimensional TE materials, and the maximum ZT is found for alloys with 12% Sb (ZT = 0.88) at 80 K.<sup>6,8</sup>

High-quality  $\text{Bi}_{1-x}\text{Sb}_x$  thin films have been prepared by electrochemical deposition in acidic aqueous solutions.<sup>9,10</sup>  $\text{Bi}_{1-x}\text{Sb}_x$  nanowire arrays have been synthesized by pressure injecting the molten alloys and direct current electrochemical deposition from toxic nonaqueous solutions of dimethyl sulfoxide (DMSO) in anodic alumina membranes (AAMs).<sup>11,12</sup> The AAM-based synthesis in conjunction with the electrochemical deposition is a widely used method to fabricate nanowires, because the AAMs possess a uniform and parallel porous structure and electrochemical deposition is a simple and inexpensive preparation technique.<sup>13–17</sup>

In this paper, high-filling, large-area, and uniform  $\text{Bi}_{1-x}\text{Sb}_x$  nanowire arrays were first electrochemically deposited into the nanochannels of AAMs from nontoxic aqueous solutions using the pulsed electrochemical deposition technique.

## Experimental Section

The AAM was prepared using a two-step anodization process as described previously.<sup>18,19</sup> After the second anodization, the AAM was etched by saturated  $\text{SnCl}_4$  solution to remove the remaining aluminum. The alumina barrier layer was then dissolved in 5 wt %  $\text{H}_3\text{PO}_4$  solution at 30 °C for 40 min. Finally, a layer of Au film (about 200 nm in thickness) was sputtered onto one side of the AAM to serve as the working electrode in

a two-electrode plating cell, and a graphite plate was used as the counter electrode. The pulsed electrochemical deposition was carried out under modulated voltage control, and a potential of  $-1.1$  V was applied between the two electrodes. During the pulsed time,  $T_{\text{on}}$ , species were reduced on the pore ground. The delayed time,  $T_{\text{off}}$ , provided time for the recovery of the ion concentration. The electrolyte was prepared by dissolving respectively  $\text{BiCl}_3$  and  $\text{SbCl}_3$  in hydrochloric solution with 4 M NaCl addition in two beakers. The resulting electrolyte mixtures with different Bi/Sb ratios were obtained from the above solutions.

Power X-ray diffraction (XRD, Philips PW 1700x with Cu K $\alpha$  radiation), field-emission scanning electron microscopy (FE-SEM, JEOL JSM-6700F), and transmission electron microscopy (TEM, H-800) with selected-area electron diffraction (SAED) were used to study crystalline structures and morphologies of nanowire arrays. The chemical composition of the nanowires was determined by energy dispersive spectrometry (EDS). For XRD measurements, the overfilled nanowires on the surface of the AAM and the back Au film were mechanically polished away. For SEM imaging, the AAM was partly dissolved with 0.5 M NaOH solution and then carefully rinsed with deionized water several times. For TEM observations, the AAM was completely dissolved with 1 M NaOH solution and then rinsed with absolute ethanol.

## Results and Discussion

The typical XRD patterns of the as-prepared samples are shown in Figure 1. Figure 1a shows the XRD pattern of the  $\text{Bi}_{0.89}\text{Sb}_{0.11}$  nanowire array deposited from the solution with a Bi/Sb ratio of 5:2 together with the standard diffraction peaks of Bi (JCPDS, 85-1331). It can be seen that all peaks can be indexed to the rhombohedral space group  $R\bar{3}m$  (to which Bi, Sb, and Bi–Sb alloys belong). These peaks are shifted to higher  $2\theta$  values from the positions expected for a pure Bi sample, which is consistent with the formation of a solid solution. The sharp and narrow XRD peaks indicate that the nanowires are highly crystalline and consist of only a single compositional phase. The peak at about  $2\theta = 39.8^\circ$  is very strong as compared with other peaks, indicating a highly preferential orientation

\* Corresponding author. Fax: +86-551-5591434. E-mail: ghli@issp.ac.cn.

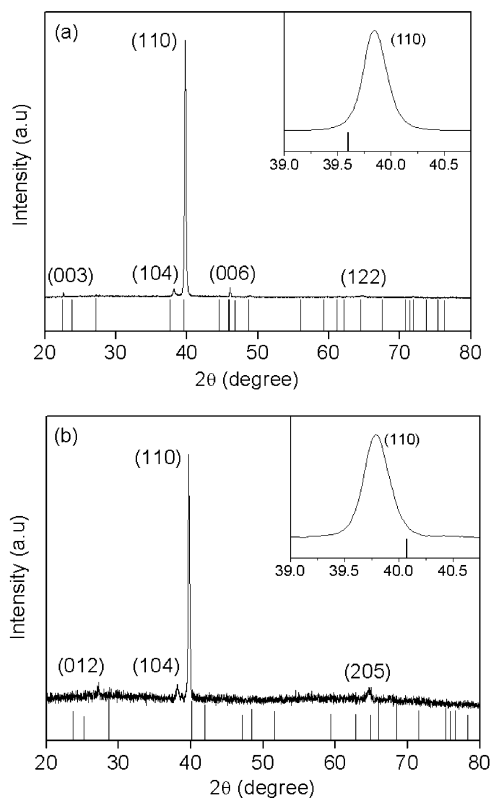


**Figure 1.** XRD patterns of 40-nm Bi/Sb nanowire arrays deposited from a bath of (a) 0.05 M Bi and 0.02 M Sb and (b) 0.02 M Bi and 0.05 M Sb. The insets show the shift of the (110) peak relative to the standard peak positions.

**TABLE 1: Atomic Percentages of Bi/Sb in  $\text{Bi}_{1-x}\text{Sb}_x$  Nanowires as a Function of Bi and Sb Concentration in the Solution**

solution concn Bi/Sb (M)	composition by EDS Bi/Sb (%)	solution concn Bi/Sb (M)	composition by EDS Bi/Sb (%)
0.05:0.01	94:6	0.04:0.05	47:53
0.05:0.02	89:11	0.02:0.05	15:85
0.05:0.03	76:24	0.01:0.05	8:92

along the [110] direction of the nanowires. Figure 1b shows the XRD pattern of the  $\text{Bi}_{0.15}\text{Sb}_{0.85}$  nanowire array deposited from the solution with a Bi/Sb ratio of 2:5 together with the standard diffraction peaks of Sb (JCPDS, 85-1324). Compared with the pure Sb sample, all the peaks are shifted to lower  $2\theta$  values as expected. The very strong intensity of the [110] peak relative to other peaks also indicates that the nanowire texture is along the [110] direction. From the XRD patterns, we have not found the presence of any Sb peaks and the shoulders in XRD peaks that were observed in the previous reported results,<sup>20</sup> which indicates that the whole electrochemical deposition process is Bi–Sb co-deposition without phase separation, and the nanowires have a homogeneous composition.

The EDS analyses indicate the nanowire compositions mainly depend on the ratio of the Bi and Sb concentrations in the electrolyte. By modulating the relative compositions of Bi and Sb in the solution, we can obtain  $\text{Bi}_{1-x}\text{Sb}_x$  alloy nanowires with  $x$  in a wide range (see Table 1).

The morphologies of the as-prepared AAM and the  $\text{Bi}_{1-x}\text{Sb}_x$  nanowire arrays are shown in Figure 2. Figure 2a is a typical SEM image of the as-prepared empty AAM. It can be seen that the AAM has a highly ordered pore arrangement with an average diameter of about 50 nm. Etching treatment in the  $\text{H}_3\text{PO}_4$  solution can widen the diameter of pores of the AAM. The

morphologies of the  $\text{Bi}_{1-x}\text{Sb}_x$  nanowire arrays after etching are presented in Figure 2b–d. Apparently, nanowires are high filling and the exposed parts of the nanowires increase as the etching time increases. As shown in Figure 2d, all the  $\text{Bi}_{1-x}\text{Sb}_x$  nanowires stand the Au cathode on the bottom of the pores and have the same length, implying that all the nanowires are deposited along the pores at the same rate.

Figure 3a shows a typical TEM image of the  $\text{Bi}_{0.89}\text{Sb}_{0.11}$  nanowires. It can be seen that the nanowires have a high aspect ratio and a smooth surface. The diameter is uniform and about 40 nm, which is smaller than that of the nanochannel of the AAM used. Previous results also show that the diameters of  $\text{Bi}_{1-x}\text{Sb}_x$  and  $\text{Bi}_{2-x}\text{Sb}_x\text{Te}_3$  nanowires are smaller than the pore diameters of the AAM and this is attributed to the presence of Sb in the nanowires.<sup>20,21</sup> However, in the present study we found that the diameters of  $\text{Bi}_{1-x}\text{Sb}_x$  and Bi ( $x = 0$ ) nanowires can be controllably modulated and increase with increasing the  $T_{\text{on}}$  and keeping the  $T_{\text{off}}$  constant, independent of the presence of Sb. Figure 3b shows the corresponding SAED pattern of the  $\text{Bi}_{1-x}\text{Sb}_x$  nanowires. The same diffraction patterns along the nanowires indicate the single-crystalline structure of the nanowires, and a single set of diffraction spots shows the (single-phase) solid solution feature of Bi–Sb alloy, which is consistent with the XRD results.

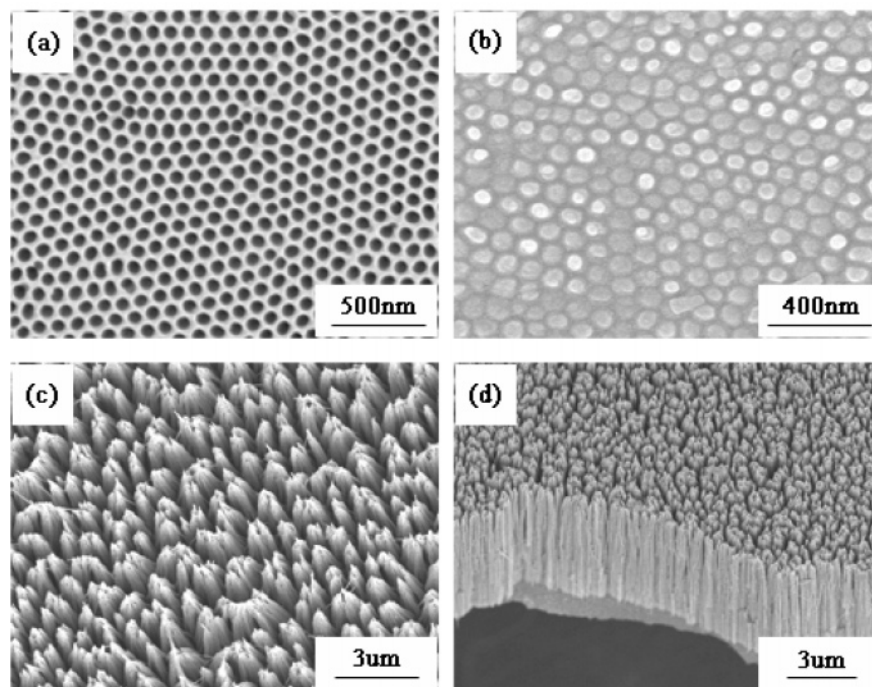
Based on this experimental result, we propose a model to explain this phenomenon. Under a short pulsed time and keeping the delayed time unchanged, the Bi ions provided for deposition in each pulse cycle are not enough to instantly cover all the area of each pore of the AAM, resulting in the growth of  $\text{Bi}_{1-x}\text{Sb}_x$  on part of the area of each pore of the AAM. At the same time, the  $\text{Bi}_{1-x}\text{Sb}_x$  ions do not have enough time to transfer along the bottom area if the delayed time is not long enough. Then the  $\text{Bi}_{1-x}\text{Sb}_x$  nanowires with a smaller diameter are formed. Contrarily, if the pulsed time is long enough to provide adequate ions,  $\text{Bi}_{1-x}\text{Sb}_x$  nanowires with the corresponding pore size of the AAM are fabricated. To further confirm this model, the following experiment was carried out.

Figure 4 shows the SEM images of  $\text{Bi}_{1-x}\text{Sb}_x$  nanowires with diameters of about 50 and 80 nm electrodeposited into the AAM with the pore size of 90 nm using  $T_{\text{on}} = 25$  ms and 40 ms with constant  $T_{\text{off}} = 50$  ms, respectively. These results indicate that  $\text{Bi}_{1-x}\text{Sb}_x$  nanowires with modulated diameters and compositions can be easily achieved by the pulsed electrochemical deposition, which provides the experimental convenience to validate the theoretical results.<sup>6,22–23</sup>

Simple electrochemical calculation indicates that the formation of  $\text{Bi}_{1-x}\text{Sb}_x$  alloy can be realized by using the present experimental conditions. To ensure the stability and solubility of  $\text{Sb}^{3+}$  and  $\text{Bi}^{3+}$  solutions and to compensate for the difference in deposition potentials of the two components, a high concentration of NaCl containing hydrochloric acid was used to form chloride complexes. The standard potentials for the bismuth and antimony chloride complexes,  $\varphi^{\ominus}_{\text{MCl}_n^{3-n}/\text{M}}$ , are related to the standard potentials of the uncomplexed  $\text{Bi}^{3+}$  and  $\text{Sb}^{3+}$  ions,  $\varphi^{\ominus}_{\text{M}^{3+}/\text{M}}$ , through their respective stability constants  $\beta_n$  at 298 K,<sup>24–25</sup>

$$\varphi^{\ominus}_{\text{MCl}_n^{3-n}/\text{M}} = \varphi^{\ominus}_{\text{M}^{3+}/\text{M}} - \frac{RT}{3F} \log \beta_n = \varphi^{\ominus}_{\text{M}^{3+}/\text{M}} - 0.0197 \log \beta_n \quad (1)$$

where M = Bi or Sb. Well-defined values of the standard potentials for the  $\text{Bi}^{3+}/\text{Bi}$  and  $\text{Sb}^{3+}/\text{Sb}$  couples are not available in the literature and are obtained indirectly through the measure-



**Figure 2.** SEM photographs of AAM and Bi-Sb nanowire arrays. (a) Typical SEM image of AAM. (b–d) Surface and cross-sectional views of Bi-Sb nanowire arrays after etching times of 2, 5, and 10 min, respectively.

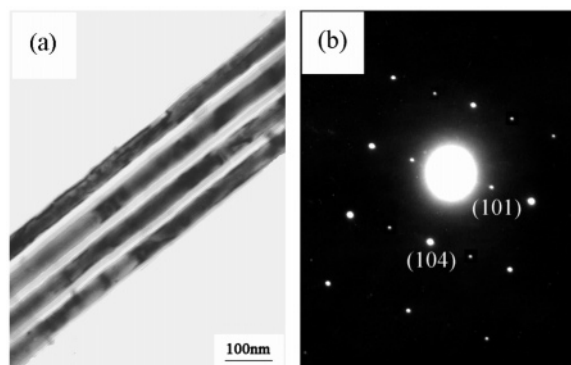


**Figure 3.** (a) TEM image of Bi-Sb nanowires. (b) Corresponding SAED pattern, revealing the nanowire is single phase.

ments of their compounds and subsequent thermodynamic calculations.<sup>26</sup>

For the  $\text{BiCl}_4^-/\text{Bi}$  and  $\text{SbCl}_4^-/\text{Sb}$  equilibrium,



the standard potentials  $\varphi_{\text{BiCl}_4^-/\text{Bi}}^\ominus$  and  $\varphi_{\text{SbCl}_4^-/\text{Sb}}^\ominus$ , calculated indirectly from the oxychloride compound, are 0.16 and 0.17 V (standard hydrogen electrode (SHE)).<sup>24,27</sup> The standard potentials for the  $\text{Bi}^{3+}/\text{Bi}$  and  $\text{Sb}^{3+}/\text{Sb}$ ,  $\varphi_{\text{Bi}^{3+}/\text{Bi}}^\ominus$  and  $\varphi_{\text{Sb}^{3+}/\text{Sb}}^\ominus$ , calculated from the standard potentials of the tetrachloro complexes and their stability constants  $\beta_4$  using eq 1 are 0.28 and 0.26 V (SHE). The standard potentials for the different  $\text{BiCl}_n^{3-n}$  and  $\text{SbCl}_n^{3-n}$  species can be calculated from eq 1, and the results are summarized in Table 2. It can be seen that the standard potentials for the different chloride complexes of both elements are very close, indicating that bismuth and antimony will co-deposit as an alloy.

Recent results show that the pulsed electrodeposition technique has become a most efficient method for the growth of uniform and continuous nanowires in the AAM, which allows

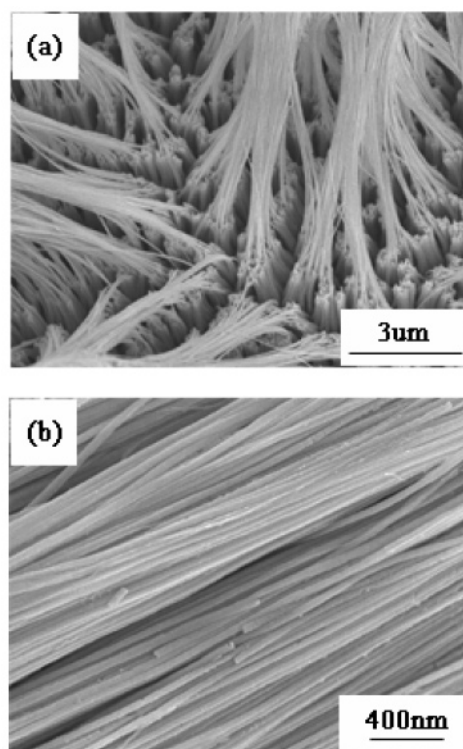


**Figure 4.** SEM images of Bi-Sb nanowires with diameters of (a) 50 nm and (b) 80 nm fabricated with  $T_{\text{on}} = 25$  and 40 ms, respectively, keeping  $T_{\text{off}} = 50$  ms in an AAM with a 90 nm pore size.

better control over the deposition parameters, such as deposition rate and ion concentration at the deposition interface, compared with the direct and alternating current deposition.<sup>28,29</sup> In our experiment, the pulsed time in each pulse cycle was so short and only a small number of metal ions at the interfaces are consumed. The delayed time provided time for the concentrations of the metal ions at the pore tips to achieve steady state through diffusion. No evident concentration gradient near the



**TABLE 2: Standard Potentials  $\varphi^{\ominus}_{\text{MCl}_n^{3-n}/\text{M}}$  (V vs SHE) for Uncomplexed Metal Ions ( $n = 0$ ) and Metal Chloride Complexes (for  $1 \leq n \leq 6$ ) Obtained from Equation 1 and the Stability Constants  $\beta_n$**

	$\text{MCl}_n^{3-n} + 3\text{e}^- \leftrightarrow \text{M} + n\text{Cl}^-$						
	$n = 0$	$n = 1$	$n = 2$	$n = 3$	$n = 4$	$n = 5$	$n = 6$
$U^{\ominus}_{\text{BiCl}_n^{3-n}/\text{Bi}}$	0.28	0.23	0.21	0.17	0.16	0.15	0.15
$U^{\ominus}_{\text{SbCl}_n^{3-n}/\text{Sb}}$	0.26	0.22	0.19	0.19	0.17	0.17	0.18

reaction interface exists during the deposition and the pulsed time controls the atom-by-atom deposition of nanowires, which improves the homogeneity of the deposition and makes the deposited nanowires have a highly preferential orientation.

## Conclusion

In summary, high-filling and ordered  $\text{Bi}_{1-x}\text{Sb}_x$  nanowire arrays have been successfully prepared from aqueous solutions by pulsed electrochemical deposition into the pores of AAMs at room temperature. The nanowires are highly crystalline and have a preferential orientation along the [110] direction. The diameters of nanowires can be modulated by changing the negative pulsed time  $T_{\text{on}}$  and keeping the delayed time  $T_{\text{off}}$  constant. The compositions of nanowires can be tuned by changing the solution concentrations. These results provide an easy route to fabricate  $\text{Bi}_{1-x}\text{Sb}_x$  nanowire arrays with different diameters and compositions that can be used to study thermoelectric properties.

**Acknowledgment.** This work was supported by the National Major Project of Fundamental Research for Nanomaterials and Nanostructures and in part by the National Natural Science Foundation of China.

## References and Notes

- (1) Hicks, L. D.; Dresselhaus, M. S. *Phys. Rev. B* **1993**, 63, 3230.
- (2) Hicks, L. D.; Harman, T. C.; Sun, X.; Dresselhaus, M. S. *Phys. Rev. B* **1996**, 53, 10493.
- (3) Venkatasubramanian, R.; Siivola, E.; Colpitts, T.; O'Quinn, B. *Nature* **2001**, 413, 597.
- (4) Lin, Y. M.; Sun, X.; Dresselhaus, M. S. *Phys. Rev. B* **2000**, 62, 4610.

- (5) Sun, X.; Zhang, Z.; Dresselhaus, M. S. *Appl. Phys. Lett.* **1999**, 74, 4005.
- (6) Rabin, O.; Lin, Y. M.; Dresselhaus, M. S. *Appl. Phys. Lett.* **2001**, 79, 81.
- (7) Lenoir, B.; Cassart, M.; Michenaud, J. P.; Scherret, H.; Scherret, S. *J. Phys. Chem. Solids* **1996**, 57, 89.
- (8) Cho, S. L.; Divenere, A.; Wong, G. K.; Ketterson, J. B.; Meyer, J. R. *J. Vac. Sci. Technol., A* **1999**, 17, 9.
- (9) Besse, F.; Boulanger, C.; Lecuire, J. M. *J. Appl. Electrochem.* **1990**, 20, 868.
- (10) Povetkin, V.; Shibleva, T.; Kovenskii, M. *Elektrokhimiza* **1990**, 26, 1616.
- (11) Lin, Y. M.; Cronin, S. B.; Rabin, O.; Heremans, J.; Dresselhaus, M. S.; Ying, J. Y. *Mater. Res. Soc. Symp. Proc.* **2001**, 635, C4301.
- (12) Prieto, A. L.; Martin-Gonzalez, M.; Keyani, J.; Gronskey, R.; Sands, T.; Stacy, A. M. *J. Am. Chem. Soc.* **2003**, 125, 2388.
- (13) Guo, Y. G.; Wan, L. J.; Bai, C. L. *J. Phys. Chem. B* **2003**, 107, 5441.
- (14) Xu, D. S.; Xu, Y. J.; Chen, D. P.; Guo, G. L.; Gui, L. L.; Tang, Y. Q. *Adv. Mater.* **2000**, 12, 520.
- (15) Xu, D. S.; Shi, X. S.; Guo, G. L.; Gui, L. L.; Tang, Y. Q. *J. Phys. Chem. B* **2000**, 104, 5061.
- (16) Choi, J.; Sauer, G.; Nielsch, K.; Wehrspohn, R. B.; Gösele, U. *Chem. Mater.* **2003**, 15, 776.
- (17) Sauer, G.; Brehm, G.; Schneider, S.; Nielsch, K.; Wehrspohn, R. B.; Choi, J.; Hofmeister, H.; Gösele, U. *J. Appl. Phys.* **2002**, 91, 3243.
- (18) Sander, M. S.; Gronskey, R.; Sands, T.; Stacy, A. M. *Chem. Mater.* **2003**, 15, 335.
- (19) Masuda, H.; Fukuda, K. *Science* **1995**, 268, 1466.
- (20) Martin-Gonzalez, M.; Prieto, A. L.; Knox, M. S.; Gronskey, R.; Sands, T.; Stacy, A. M. *Chem. Mater.* **2003**, 15, 1676.
- (21) Martin-Gonzalez, M.; Prieto, A. L.; Gronskey, R.; Sands, T.; Stacy, A. M. *Adv. Mater.* **2003**, 15, 1003.
- (22) Lin, Y. M.; Rabin, O.; Cronin, S. B.; Ying, J. Y.; Dresselhaus, M. S. *Appl. Phys. Lett.* **2002**, 81, 2403.
- (23) Lin, Y. M.; Cronin, S. B.; Rabin, O.; Ying, J. Y.; Dresselhaus, M. S. *Appl. Phys. Lett.* **2001**, 79, 677.
- (24) Bard, A. J.; Parsons, R.; Jordan, J. *Standard Potentials in Aqueous Solution*; Marcel Dekker: New York, 1985.
- (25) Pantani, F.; Desideri, P. G. *Gazzetta* **1959**, 89, 1360.
- (26) Bard, A. J. *Encyclopedia of Electrochemistry of the Elements*; Marcel Dekker: New York, 1973; Vol. IXB.
- (27) Milazzo, G.; Caroli, S. *Tables of Standard Electrode Potentials*; Wiley: New York, 1978.
- (28) Nielsch, K.; Müller, F.; Li, A. P.; Gösele, U. *Adv. Mater.* **2000**, 12, 582.
- (29) Guo, Y. G.; Wan, L. J.; Zhu, C. F.; Yang, D. L.; Chen, D. M.; Bai, C. L. *Chem. Mater.* **2003**, 15, 664.